

Proceeding Paper

Decisive Effect of Gas Metal Arc Welding-Based Additive Manufacturing on the Bead Profile, Microstructure and Tensile Properties of Ni-Cr-Mo Components [†]

Aghesha M. Alwyn, A. K. Lakshminarayanan * and S. R. Koteswara Rao

Department of Mechanical Engineering, Sri Sivasubramaniya Nadar College of Engineering, Kalavakkam 603110, Tamil Nadu, India; aghesham@ssn.edu.in (A.M.A.); koteswararaosr@ssn.edu.in (S.R.K.R.)

* Correspondence: lakshminarayananak@ssn.edu.in

[†] Presented at the International Conference on Processing and Performance of Materials, Chennai, India, 2–3 March 2023.

Abstract: This study focuses on metal inert gas welding for nickel alloy additive manufacturing using both cold metal transfer (CMT) and pulse multi control (PMT). For both single- and dual-bead deposition, the key parameters (current, travel speed, feed, weave, and height offset) were tuned. A hollow square component of 20 mm in height, 60 mm side length, and 16 mm width was created using these measurements. A macrostructural study demonstrated that flawless accuracy in geometry was attained by both PMT and CMT. In comparison to PMT, CMT specimens showed increased interlayer hardness but decreased hardness in the deposited layers. These changes were explained by modifications in eutectic phase size, distribution, and partial dissolution at the contact. For the wire arc additive manufacturing of nickel alloy components, pulse multi control is preferred over cold metal transfer.

Keywords: nickel alloy; wire arc additive manufacturing; cold metal transfer; pulse multi control; microstructure; hardness



Citation: Alwyn, A.M.; Lakshminarayanan, A.K.; Rao, S.R.K. Decisive Effect of Gas Metal Arc Welding-Based Additive Manufacturing on the Bead Profile, Microstructure and Tensile Properties of Ni-Cr-Mo Components. *Eng. Proc.* **2024**, *61*, 10. <https://doi.org/10.3390/engproc2024061010>

Academic Editors: K. Babu, Anirudh Venkatraman Krishnan, K. Jayakumar and M. Dhananchezian

Published: 26 January 2024



Copyright: © 2024 by the authors. Licensee MDPI, Basel, Switzerland. This article is an open access article distributed under the terms and conditions of the Creative Commons Attribution (CC BY) license (<https://creativecommons.org/licenses/by/4.0/>).

1. Introduction

Superalloys based on nickel have outstanding mechanical strength, superior surface stability, resistance to oxidation, and resistance to thermal deformation. Because of their exceptional mechanical strength and resilience to creep and corrosion in challenging conditions, Inconel alloys are referred to as superalloys. Because of its exceptional age-hardened strength at both room temperature and high temperatures, along with its resistance to corrosion, Inconel 625 has found extensive and varied uses in the aerospace, maritime service, and petrochemical industries [1]. In the aerospace industry, tubing used for shroud rings, spray bars, fuel and hydraulic lines, and exhaust and thrust systems are just a few examples of components where Inconel 625 is used [2]. Eventually, because Inconel 625 can withstand corrosion from seawater, it is widely used in the nuclear and marine industries [3]. Numerous traditional manufacturing techniques, including melting and solidification processes, spray forming, cladding, bimetallic extrusion of components, and powder metallurgy have been used to create Inconel 625 components [4]. Unfortunately, a lot of products made using Inconel 625 have intricate shapes, making conventional fabrication exceedingly costly. AM fabrication with Inconel 625 has become a viable technique for part production as the demand for the technology continues to expand and increase. The current work uses the CMT and PMC methods to build the component on a nickel alloy 718 base substrate utilizing nickel alloy wire 625.

2. Experimental Work

Inconel 718 (10 mm plate) and Inconel 625 (1.2 mm wire) were used in this investigation to fabricate a structure. For deposition, the Fronius TPS 400 I MiG welding equipment was

used, utilizing PMC and CMT procedures. Trial runs were carried out before manufacture to optimize the process parameters. During the testing runs, beads with the labels 1–7 (CMT) and a–g (PMC) were made on an Inconel 718 plate (100 × 100 sq. mm) (Figure 1). To finalize the process parameters, Bead-7 (CMT) and Bead g (PMC) were selected based on their desirable bead shape. Layer by layer, the fabrication process was carried out, with each layer consisting of four CMT and three PMC passes that deposited metal with a breadth of about three to four millimetres apiece. To achieve the required height, five layers were layered. The specific criteria for CMT/PMC are presented in Table 1.

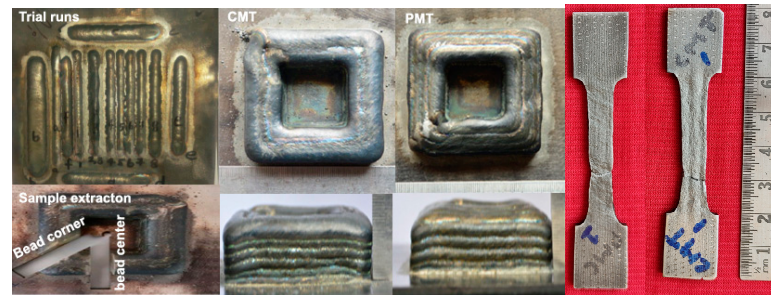


Figure 1. Trial runs; fabricated components and tensile sample after testing.

Table 1. Deposition variables used.

Sample	Current (A)	Voltage (V)	Travel Speed (cm/min)	Wire Feed Rate (mm/min)	Weave (mm)
CMT	138	13.2	25	5.4	2
PMC	115	20.7	30	4.9	0.5

Weld direction was maintained clockwise, and weave parameters were changed in-pass for shape. Figure 1 shows the appearance of the finished component, and specimens from each component were cut using WEDM. The cross-sections of the macrostructure and microstructure were captured using an optical microscope examination after being polished and etched with Nital. The tensile properties and microhardness at different locations in both samples were obtained to analyze the heterogeneity within the components.

3. Results and Discussion

3.1. Macrostructure and Microstructure of CMT and PMC Samples

The cross-sectional macrostructure reveals layer-by-layer deposition patterns. The PMC specimens exhibit superior penetration between passes compared to CMT, with well-shaped edges, while CMT specimens show bulging and poorly shaped edges. PMC also achieves deeper penetration into the base nickel alloy 718, which is evident at the base metal and deposited bead interface (Figure 2a,b). Microstructure analysis shows varying grain structure and size from the middle of the side arm to its corner and between CMT and PMC. Both exhibit finely intermixed dendritic and cellular microstructures at certain locations (Figure 2c,d). However, in CMT, columnar dendrites below each layer, due to directional growth against the heat flux, are observed (Figure 2f,g). Local cooling rates during solidification have an impact on the transverse section microstructure at different locations [5]. Due to improved melt pool control provided by current pulsing, fine grains were found in PMC. Every layer has cellular or cellular dendritic structures at the top and primarily columnar dendritic structures with varying-sized grains at the bottom. The change in microstructure from completely columnar to cellular/cellular dendritic results from decreased cooling rates from the bottom to the uppermost portion of the melt pool (Figure 2e) [6].

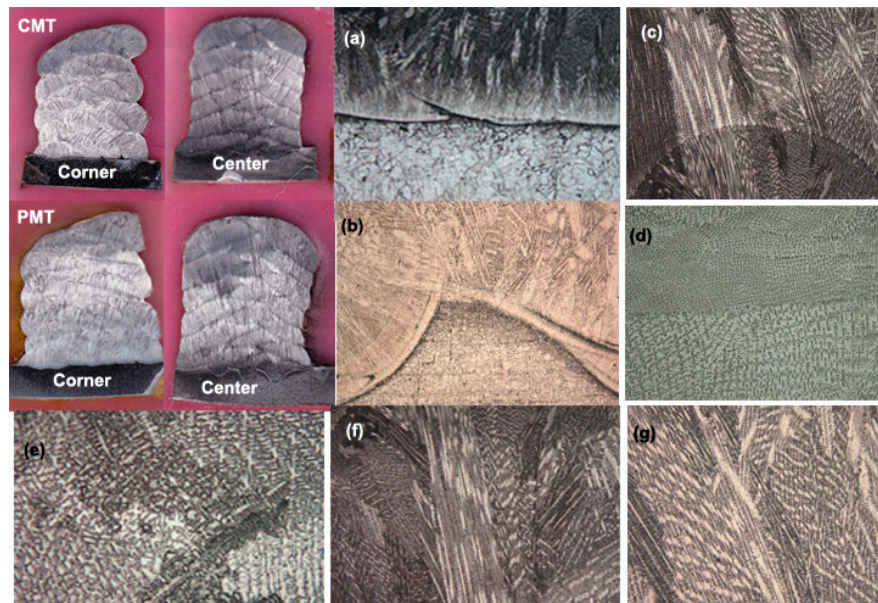


Figure 2. Macrostructure and microstructure of different zones of CMT and PMC samples. (a) bead interface CMT (b) bead interface PMC (c), (d) microstructure morphology PMC (e,f) cellular microstructure morphology CMT (g) columnar dendrites – CMT.

3.2. Mechanical Properties and Heterogeneity Index

Based on a closer look at Table 2, it is clear that the CMT sample has a considerably greater tensile strength—760 MPa— 4% more than the PMC sample. In contrast, it is found that the CMT sample’s ductility is 36%, which is 16% less than that of the PMC sample. Interestingly, there is a notable resemblance between the average hardness values of both samples despite these differences in tensile strength and ductility. Equations (1) and (2), respectively, were used to calculate the microhardness inhomogeneity and tensile anisotropy index numbers to comprehend the change in tensile property and microhardness values with regard to build orientations and are presented in Table 2.

$$\delta_{hardness} = \frac{H_{max} - H_{min}}{H_{avg}} \tag{1}$$

$$\delta_{tensile} = \frac{\sigma_{max} - \sigma_{min}}{\sigma_{avg}} \tag{2}$$

Table 2. Tensile strength, microhardness, anisotropy and inhomogeneity index.

Sample	Tensile Strength (MPa)	% Elongation	Microhardness (HV _{0.05})	Strength Anisotropy Index	Microhardness Inhomogeneity Index
CMT	760	36	260	10.52	11.11
PMC	730	42	250	6.84	8.00

The results unambiguously show that the CMT sample has a greater tensile anisotropy index (53.84%) than the PMC sample. Likewise, the CMT sample’s microhardness inhomogeneity index is 38.9% greater than the PMC sample. These results can be explained by the microstructural differences in the manufactured samples at various points. Because most sections of the PMC sample have a mixed microstructure with fine cellular and dendritic formations that line up with the build orientation, the sample is more homogeneous and less anisotropic. On the other hand, the coarser dendritic and columnar structure of the CMT sample is reflected in its greater anisotropy index and increased

inhomogeneity index. The associations discovered by Yangfan et al. [7] in CMT-fabricated nickel 625 alloy are consistent with the correlations found here between the microstructure and mechanical characteristics.

4. Conclusions

In this study, it is observed that PMC is more promising than CMT as a process for additive manufacturing of Inconel 625. In contrast, the lack of fusion and sub-optimal bead deposit structure makes the CMT build less desirable. In contrast, hardness readings do not show any variation in the process, which suggests a uniform surface structure. The microstructure comparison of CMT and PMC shows variations in the arrangement of dendritic and cellular structures. In addition, there is less melting of previous beads and penetration in CMT compared to PMC. PMC also offers better shape and dimension control compared to the CMT process.

Author Contributions: Conceptualization, methodology, original draft preparation, A.K.L.; formal analysis and investigation, A.M.A.; validation, S.R.K.R. All authors have read and agreed to the published version of the manuscript.

Funding: This research received no external funding.

Institutional Review Board Statement: Not applicable.

Informed Consent Statement: Not applicable.

Data Availability Statement: Data is contained within the article.

Conflicts of Interest: The authors declare no conflict of interest.

References

1. Xu, D.; Zan, S.; Liao, Z.; Yang, Y.; Gao, Y.; Fu, M. Investigation of surface integrity in grinding of nickel based superalloy under different cooling conditions. *J. Manuf. Process.* **2022**, *107*, 240–251. [[CrossRef](#)]
2. Gonzalez, J.A.; Mireles, J.; Stafford, S.W.; Perez, M.A.; Terrazas, C.A.; Wicker, R.B. Characterization of Inconel 625 fabricated using powder-bed-based additive manufacturing technologies. *J. Mater. Process. Technol.* **2019**, *264*, 200–210. [[CrossRef](#)]
3. Kawasaki, K. High-speed milling of Inconel 625 alloy using carbide ball end mills. *J. Mech. Sci. Technol.* **2022**, *36*, 6239–6245. [[CrossRef](#)]
4. Savinov, R.; Wang, Y.; Shi, J. Evaluation of microstructure, mechanical properties, and corrosion resistance for Ti-doped inconel 625 alloy produced by laser directed energy deposition. *Mater. Sci. Eng. A* **2023**, *884*, 145542. [[CrossRef](#)]
5. Yangfan, W.; Xizhang, C. Investigation on the microstructure and corrosion properties of Inconel 625 alloy fabricated by wire arc additive manufacturing. *Mater. Res. Express* **2023**, *6*, 106568. [[CrossRef](#)]
6. Cheepu, M.; Lee, C.I.; Cho, S.M. Microstructural Characteristics of Wire Arc Additive Manufacturing with Inconel 625 by Super-TIG Welding. *Trans. Indian Inst. Met.* **2020**, *73*, 1475–1479. [[CrossRef](#)]
7. Yangfan, W.; Xizhang, C.; Chuanchu, S. Microstructure and mechanical properties of Inconel 625 fabricated by wire-arc additive manufacturing. *Surf. Coat. Technol.* **2019**, *374*, 116–123. [[CrossRef](#)]

Disclaimer/Publisher's Note: The statements, opinions and data contained in all publications are solely those of the individual author(s) and contributor(s) and not of MDPI and/or the editor(s). MDPI and/or the editor(s) disclaim responsibility for any injury to people or property resulting from any ideas, methods, instructions or products referred to in the content.